Spring for clapping X-wing Micro Air Vehicles

Yao-Wei Chin, Yu-Kai Luo, Zi-Yuan Ang, and Gih-Keong Lau

School of Mechanical and Aerospace Engineering, Nanyang Technological University, Singapore 639798

Abstract

Four-winged ornithopters like Delfly make use of clap and fling to enhance thrust generation. Yet, clapping of the four wings (forming a cross) requires high energetic cost and their wing kinetic energy is not recovered using rigid-body mechanism. To help recover the wings' kinetic energy, we designed and developed a compact T-shaped elastic flexures, replacing a pivot revolute joint for this X-wing micro air vehicles (MAV). The elastic mechanism is made of flexible polyimide film and rigid carbon fiber plates. The polyimide film is capable of storing elastic strain energy for large bending. Higher elastic storage in the film hinges improved the clapping speed of the X-wing flapper to generate higher thrust without incurring additional energetic costs. Hence, it is useful to enhance the thrust of low-frequency clappers. This X-wing clapper of a 13.4g total weight is able to generate thrust up to 20.7g force and demonstrates tethered hovering and climbing.

1 Introduction

Dragonfly are agile flyers which have two wing pairs in tandem. Their four-wing configuration inspired man-made flapping-wing flight vehicles or ornithopters with four wings. The four wings are two criss-cross wing planes. When the two criss-crossing wing planes are opened, their leading edges crosses like an X. When the two wing planes are close, their two leading edges becomes parallel and their wing foils overlap. Examples of the X-wing ornithopter include the Luna [1], which is powered by a long twisted rubber band, and the DelFly [2], which is powered by an electric motor. Four-winged ornithopters have good flight stability by moving the two pairs of wings in countering directions, minimizing the body rocking [2]. In contrast, two-winged ornithopters are more prone to body rocking due to asymmetric inertial force induced by flapping wings.

Typically, an electric motor via a double crank mechanism was used to drive a scissor-like bi-plane or X wing clappers, such as Delfly or Silverlit Wing-Master I-Bird. Two pairs of X wings claps together once or twice during either ends of wing stroke. For example, X-wing Delfly adopted the clap-and-fling mechanism to increase the thrust-power ratio (a measure of efficiency) by about 50% [2, 3]. Each of the two wing planes is pivoted about a center revolute joint, which consists of a hollow sleeve and a pin shaft. Such joint is subjected to friction and unable to store elastic energy. One possible solution is to use elastic elements to convert the kinetic energy of the wings into elastic energy which is subsequently recovered during stroke reversal.

Elastic energy storage has been used in non-clap two-winged ornithopters for power saving [4, 5]. For example, Baek and Fearing [5] integrated a discrete helical spring to the crank-slider mechanism for two flapping wings and showed experimentally that the measured power saving is as much as 19%, near the resonant frequency [5]. However, there was no compact spring to be integrated into the limited space at the pivot of the four-winged clapping mechanism. Traditional cross flexures take space more than a pivot does. Hence, the objective of this research is to develop a compact flexural mechanism to help recover wing kinetic energy and assist faster clapping of X-wing FWMAV. In this way, the X-wing FWMAV should be more energy efficient while maintaining or even improving its thrust generating capability.

Hovering is a challenge for FWMAV because the wings have to beat fast and large stroke to produce sufficient thrust to lift its weight. Heavier FWMAVs must either beat larger wings or beat wings faster to hover, hence expends much higher kinetic energy. Elastic energy storage is in need to recover the higher wings' kinetic energy by using stiffer spring. Yet there are challenges to design a compact, stiff, yet durable spring for the X-wing FWMAV because the large-stroke bending and high reciprocating torque may break the elastic hinges.

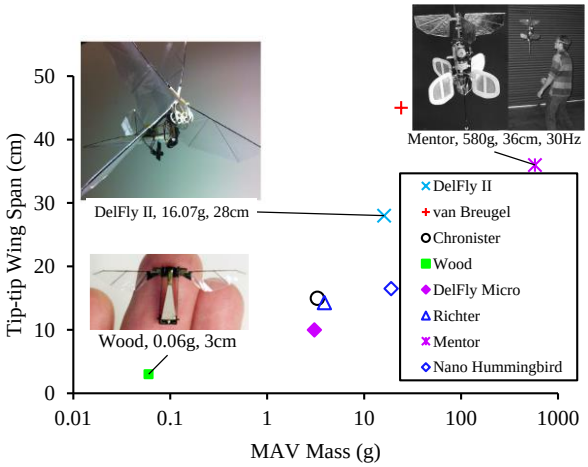

Figure 1 Wingspan and mass of flapping wing micro air vehicles reported or claimed to hover or fly slowly, from [1] [6] [7] [8] [9] [10].

2 Principle and Design

Flight by flapping wings was expected to consume more energy than rotary flight because kinetic energy of flapping wings is lost within a quarter cycle of acceleration and deceleration. In a quarter wing-beat cycle, motor accelerates the wings to maximum angular speed with maximum wings' kinetic energy at the mid stroke. However, this wing kinetic energy is lost when motor decelerates the wings to a stop at the wing's extreme position.

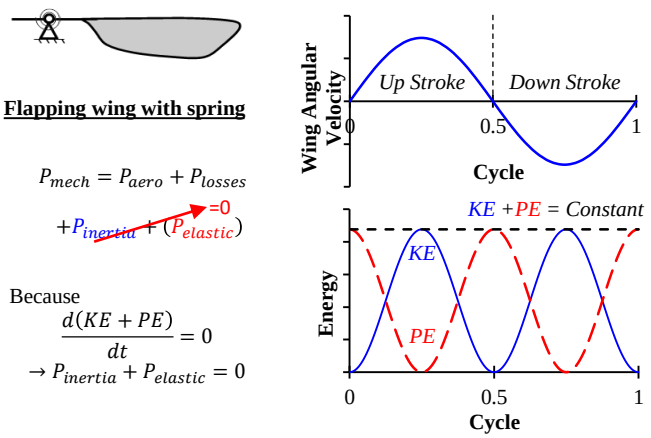

Figure 2 Kinetic energy (KE) lost in wing reciprocation can be recovered with spring hinge that can store equivalent elastic energy (PE).

The loss of wing kinetic energy can be stored as elastic energy in a spring hinge for wings instead. The spring hinge recovers kinetic energy when it elastically deforms from neutral mid stroke to slow down the wing towards end stroke. In a subsequent quarter stroke, its energy release assist the wing reversal to mid stroke. For full energy recovery, the capacity of elastic storage (i.e. of spring) needs to match the wings' maximum kinetic energy change. For a wing of rotation inertia J_0, which beats sinusoidally with a stroke of ϕ at a wingbeat frequency f, its maximum kinetic change over a quarter wingbeat cycle is:

$$\mathrm{KE}_{wing,max} = \frac{1}{2}\pi^2\phi^2 f^2 J_0 \qquad (1)$$

A wingbeat cycle of the X-wing consists of clap and fling strokes. The wing kinematic varies over the quarter cycles of clapping and flapping. More specifically, the maximum wing speed of the clapping quarter cycle is different from that of the flinging quarter cycle. This is due to the non-linear crank-rocker drive and elastic hinge assistance. The total kinetic energy change over a wingbeat cycle is a sum of the kinetic energy changes during the wing clapping and during the wing flinging:

$$Total\ \mathrm{KE}_{wing,max} = \frac{1}{2}J_0\left(\omega^2_{max,clap} + \omega^2_{max,fling}\right) \qquad (2)$$

Spring design is not trivial work for an X-wing clapping mechanism. The spring must be compact, lightweight and tough enough. Coil springs are not suitable because they take up too much space. Instead, frictionless leaf springs like film flexures are more suitable to replace revolute joints. To enable large wing stroke, the flexural hinges need to bend more than 90° without breaking. Thin metal sheet, which made stiff springs, break when subjected to such a large angle of bending. Flexible polyimide film hinge bordered by rigid plates of carbon fiber reinforced polymer were found useful for Robobee [11] [7] [12] of less than 12cm wing span. It was not clear if the film hinges can be scaled up to store more elastic storage for larger FWMAV [13] of greater than 24cm wing span. This work shows that polyimide film hinges work for greater-span wings and can store elastic storage for X wing (two cross wing planes) when the hinges are configured in a compact T shape (see Figure 3).

The T-shaped compliant mechanism consists of a mirror-pair of polyimide flexural hinges. Each polyimide hinge connects two rigid plates, namely a wing base and a vertical ground. The polyimide hinge acts a frictionless pivot for the wing base, which swings about the vertical ground at the symmetry plane. Each wing base carries a wing plane that spans both sides of the pivot. The wing plane has its leading edge of wing foil reinforced by a carbon spar. The other wing plane has it leading edge offset from the other one so that the cross spars of the two wing planes do not collide with each other.

Upon assembly, the hinges are bent 90 degrees from the vertical. Elastic recoil of the hinges assists clapping of the opposite wing planes at the horizontal plane. In the subsequent quarter stroke of flinging (reverse to clapping), a force is needed to peel the clapped wings apart and to deform the elastic hinge. While a wing rotates by an angle of θ from the horizon, the elastic flexure bends an angle of β. The elastic energy storage stored in the flexure is the work done to the flexure:

$$W_{elastic} = \int_{\beta_1}^{\beta_2} K\beta\, d\beta \qquad (3)$$

where K is the torsional stiffness of the flexure, which is the ratio of bending moment to the bending angle given as:

$$K = \frac{dM}{d\beta} = \frac{EI}{L},\ where\ I = \frac{bh^3}{12} \qquad (4)$$

where E is the Young modulus, I is the area moment of inertia, L is the length, b is the width and h is the thickness of the polyimide film used as the flexure. The polyimide film used is 0.127mm (5mil) thick Kapton HN (E=2.5 GPa).

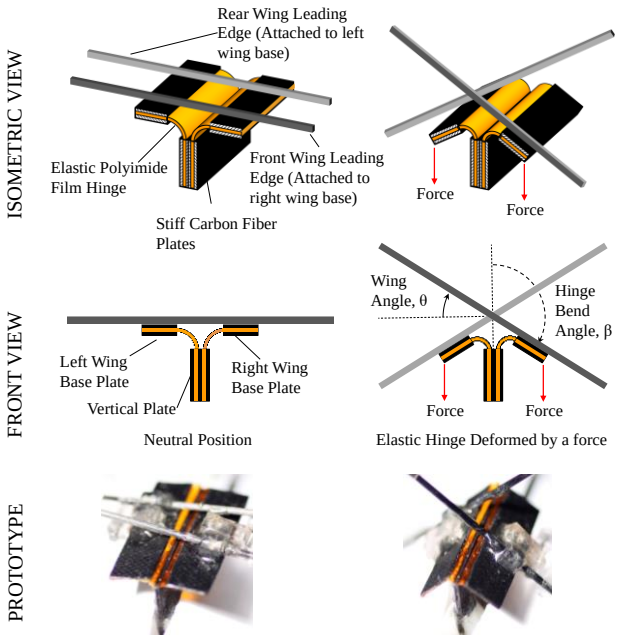

Figure 3 X-wing clapper with elastic hinge. The elastic hinge tends to return the wing base plate to vertical attitude, but is stopped at the horizontal by the opposite leading edge. As such the wings clapped together at the horizon. A force is required to rotate the wing base downwards to fling open the wings.

This elastic energy stored in the flexure is released upon reversal of the wing stroke. Release of the elastic energy speeds the wings to clap at the horizontal neutral position. The higher the elastic storage, the faster the wing claps. To show the effect of increasing elastic energy storage, we made three sets of hinges: 5 mm, 10 mm, and 20 mm, given the same 1mm hinge length (See Figure 6). Too stiff a hinge may elastically resist the start of a rotary motor.

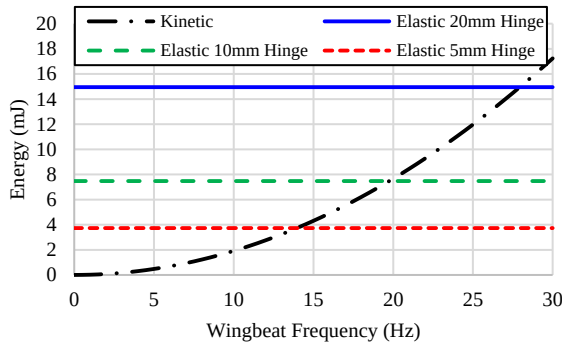

Figure 4 Calculated wing kinetic energy of a wing pair (sinusoidal wing stroke assumption) and the elastic energy storage in a single PI hinge with each different hinge width for a wing stroke of 50° from horizon.

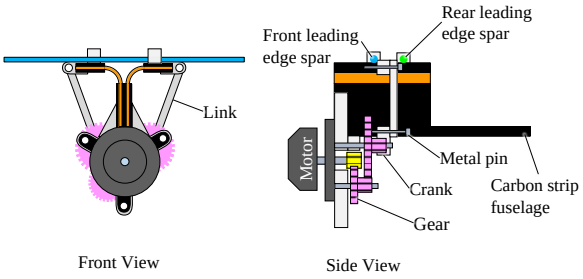

Figure 5 The double crank rocker mechanism with brushless motor and gearbox with 1:10.67 for the clapping mechanism.

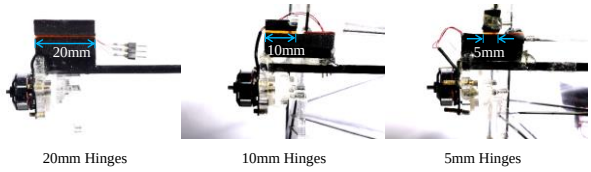

Figure 6 Elastic clappers with hinge width decreasing from 2cm to 0.5cm to show the effect of elastic stiffness.

The X-wing consists of two overlapping sheets of 25μm thick Mylar foils, which are reinforced spanwise by 1mm thick carbon rods and chordwise by 0.5mm thick carbon rods. Each sheet of foil spans the left and right sides of a middle pivot. (Figure 7a). A half of the foil has its leading edge attached to the front spar, while the other half has its leading edge attached to the rear spar. The attachment is done by slotting the rod through each foil sleeve. As the two spars criss-cross open, the foil is bent to form a V-shape about the middle pivot. (Figure 7b). The wing model in SolidWorks estimates J_0 as 5097g.mm^2 about the rotational axis at foil centre. Assuming sinusoidal wing stroke, the kinetic energy of the wings increases with the second order of wingbeat frequency according to equation (1), as shown in Figure 4.

Actuation of the wing base plates is provided through a double crank-rocker mechanism, driven by a DC brushless motor (Hobbyking AP03 7000kv) (See Figure 5). The output torque of the brushless motor is amplified 10.67 times through a speed reduction gearbox to spin the 3mm crank. The rigid linkages and the body frame to hold the gear shafts and motor are made of laser cut acrylic blocks.

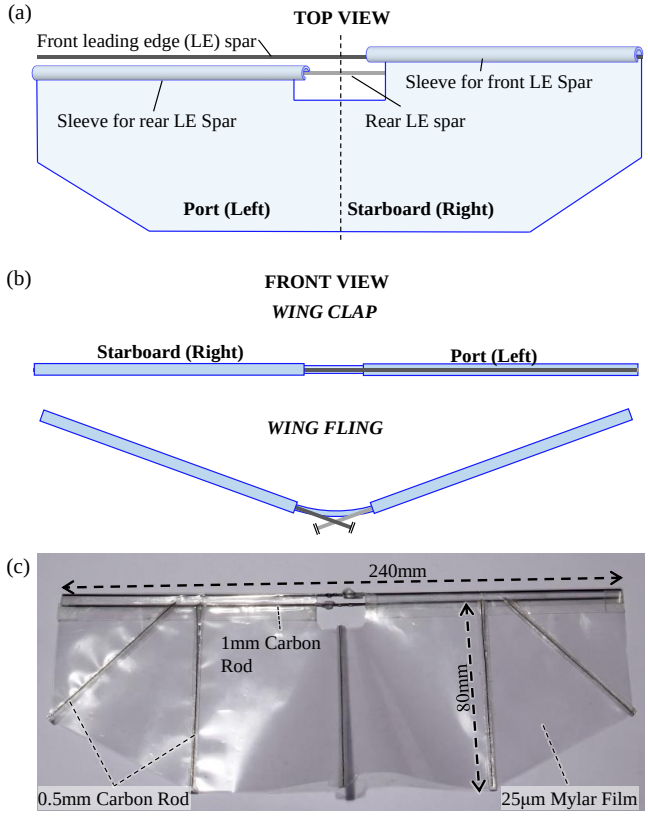

Figure 7 (a) Top view of the top wing foil design. Front LE spar is slotted into the starboard sleeve of the foil. Rear LE Spar is slotted into the port sleeve of the foil (b) Front view of the top wing foil when the wings clap and fling open. The top foil is folded to a V-shape by the LE spars. (c) X-wing with two overlapping sheets of wing foils with reinforcement spars.

3 TESTING METHODS

First the static elastic behaviour of the hinges is measured by deadweight loading on the wing leading edge at a fixed distance away from the hinge (Figure 8). The wing base was disengaged from the crank to free it from the friction of the gears and motor. Increasing weights induced a larger moment M to bend the hinge to larger angle β. This moment-angle relationship must be determined experimentally because the PI hinge yielded at large angle which was unaccounted in theory, though it maintained elasticity. This actual moment-angle relationship is used to determine the elastic energy stored:

$$W_{elastic} = \int_{\beta_1}^{\beta_2} \mathrm{M}(\beta) d\beta \qquad (5)$$

If the static load on the leading edge is removed abruptly, the elastic hinge recoils the wing towards the horizon. The stiffer hinges clap the wings faster when released from the same

deflection (40° wing angle which corresponds to a hinge bending angle of 130° bending angle). This recoil time of the hinges is observed using a high speed camera.

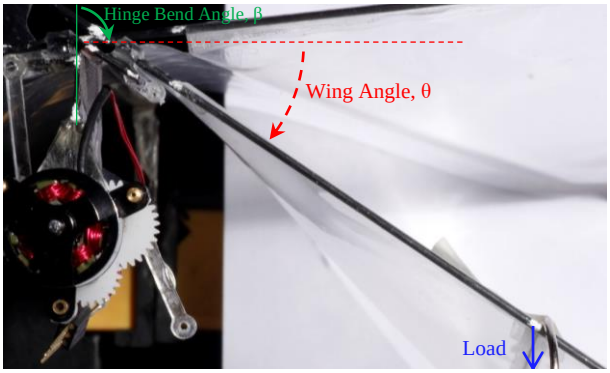

Figure 8 Static loading on the wing to determine the elastic hinge behaviour.

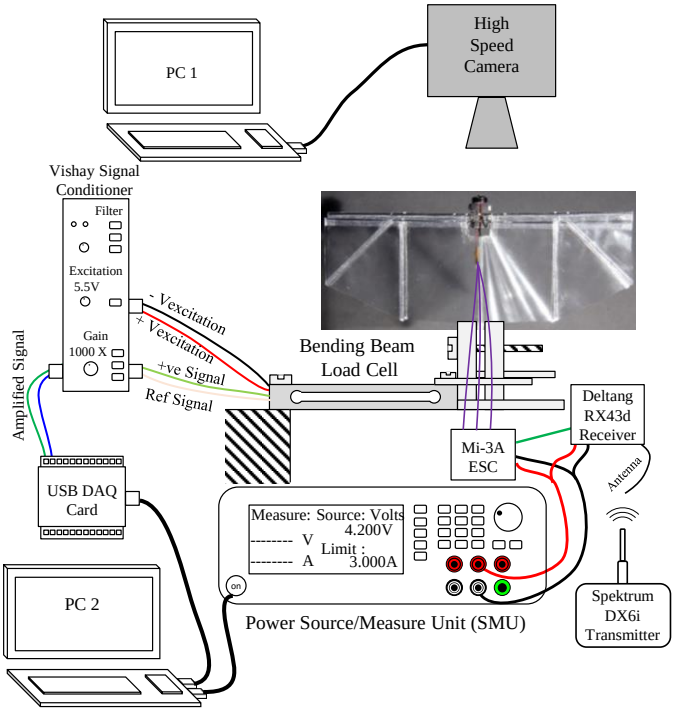

Figure 9 Tethered flight test setup for the measurement of thrust and input power to motor and high speed video of the wing kinematics.

Secondly, a tethered flight test was done by running the X-wing clapper on a load cell, as shown in Figure 9. The clapper was driven by a brushless motor which is controlled remotely with a transmitter through a receiver and electronic speed controller (ESC). A source/measure unit (Agilent B2902A SMU) provides constant-voltage power input to the ESC and receiver, and measure the supplied current simultaneously at 2000Hz sampling rate.

Simultaneously, a load cell (Zemic Q47-20*6-6, 120g capacity) was used to measure the thrust generated by the clapping wings. The output signals from the load cell were amplified 1000 times using a signal conditioner before it was logged using a data acquisition card (NI USB6009 DAQ card) at 2000Hz sampling rate.

In addition, the wing clapping motions were recorded in video of 512×512 pixels at a frame rate of 2000 frame per second using Photron FASTCAM 1024 high-speed camera. The wing leading edge motions were tracked to yield the instantaneous wing position and wing angular speed in the stroke plane, and the hinge bending angle. The vertical carbon fiber plate was also tracked to provide the correct angle reference line, because the clapper body rocked and rolled a little during wing oscillation (Figure 10).

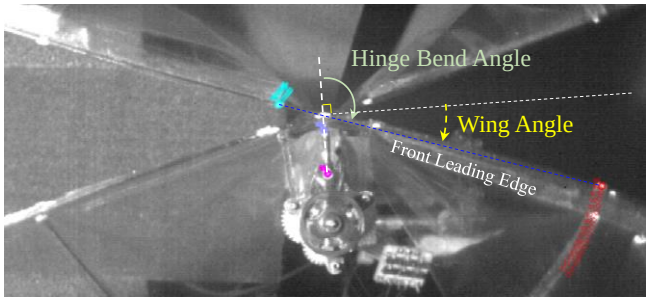

Figure 10 Tracking of the leading edge motion and vertical plate in the high speed snapshot for 2cm hinges X-wing.

4 Results and Discussions

4.1 *Elastic Hinge Behaviour*

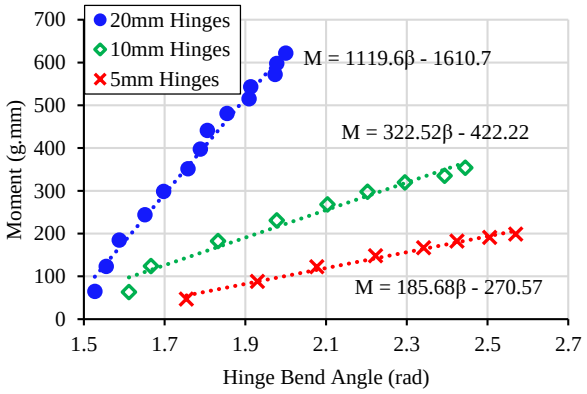

Figure 11 Bending moment required to bend the hinges.

Figure 11 shows the bending moment required to bend the hinge increases linearly with the bending angle. The 2cm hinge is almost 3.5 times stiffer than the 1cm hinge and 6 times more than the 0.5cm hinge. The elastic energy storage is proportional the stiffness. However, too much bending causes the yielding of the plastic hinge. The plastically deformed plastic hinge may not return fully upon removal of the deadweight. Yet, they exhibit consistent elastic characteristics.

The elastic energy stored is released and converted to the wing kinetic energy that assist wing clapping. In presence of air damping, the 20mm hinge carrying a wing plane (spanning over the left and right) recoiled to the 0° wing angle within 0.0765s. Similarly the 10mm hinge carrying the same wing recoil back to 0°, but slower at 0.093s. The 5mm hinge is the

slowest to recoil back for 0.1200s (see Figure 12). In the wing reciprocation, this quasi-static spring back effect would manifest in a faster wing clap than the fling.

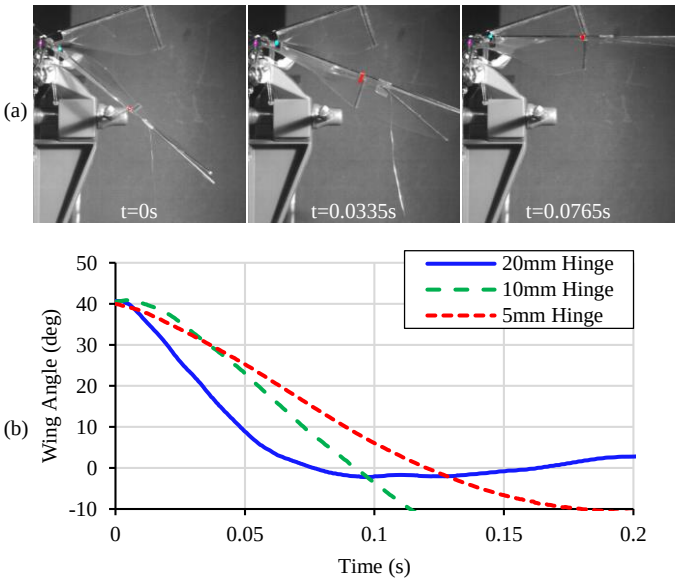

Figure 12 (a) High speed snapshot of the wing spring back for the 2cm hinge. (b) The time taken for the leading edge to return to horizontal.

4.2 *Wing Kinematics*

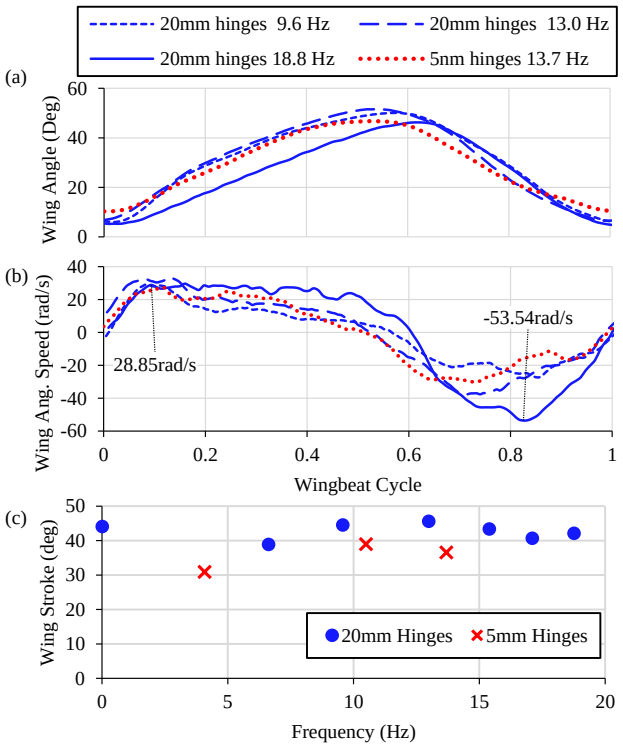

Figure 13 (a) Wing angular position and (b) Wing angular velocity in a wingbeat cycle at different wingbeat frequencies. (c) Wing stroke along wingbeat frequency for 2cm hinges and 0.5cm hinges.

During a quarter cycle of wingbeat, the elastic hinges assist the motor to clap wings faster. In a subsequent quarter cycle of wing fling, it elastically resists the wing motion. The work done by motor against the elastic hinges is stored as elastic energy, which will be released in the subsequent quarter wingbeat cycle. As a result the wing clapping is faster than the wing fling as shown in Figure 13. At first, the wings fling open with a short burst of high angular speed, but slowed down at larger wing angle. During the quarter cycle of wing fling, a part of the motor power is used to deform the elastic hinge, storing as elastic energy. With larger elastic storage, the motor clapped the wings at higher speed, and the clap duration is shorter than the fling.

As the wingbeat frequency increases, the clap peak angular speed increases significantly, but the maximum fling angular speed change slightly. Figure 14 shows that the wing kinetic energy in stroke plane increases with the wing beat frequency as shown in. The same wing on different hinges show different maximum wing kinetic energy given the same wingbeat frequency due to the impact of spring recoil on the wings' speed profile (See Figure 13b). However, the elastic energy storage remains constant because the wing stroke did not change much along frequency. At higher frequency, the wing kinetic energy increases beyond the elastic energy storage.

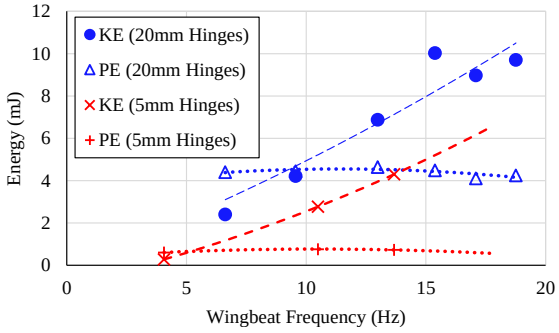

Figure 14 Total maximum kinetic energy of clap and fling stroke for a single wing pair and the elastic energy storage in a single hinge along wingbeat frequency.

4.3 *Thrust Generation and Energetic Cost*

Faster clap is useful to generate more powerful thrust, as shown in Figure 15(a). Given the same wingbeat frequency, the 20mm hinges help clap the wings faster, and thus increases the thrust generation. Stiffer hinges are good for faster clap with no extra power needed, as shown in Figure 15 (b). This showed that elastic energy storage primarily boosted the wing clapping speed for larger thrust generation given same wingbeat frequency. Hence, the optimal elastic hinges improved the efficiency of the thrust generation.

At a maximum thrust of 20.7g, the X-wing with 2cm hinges is able to produce sufficient thrust to lift off and climb. In a tethered flight with onboard ESC, receivers and battery, the X-wing could lift its weight of 13.4g and climb, as shown in Figure 17.

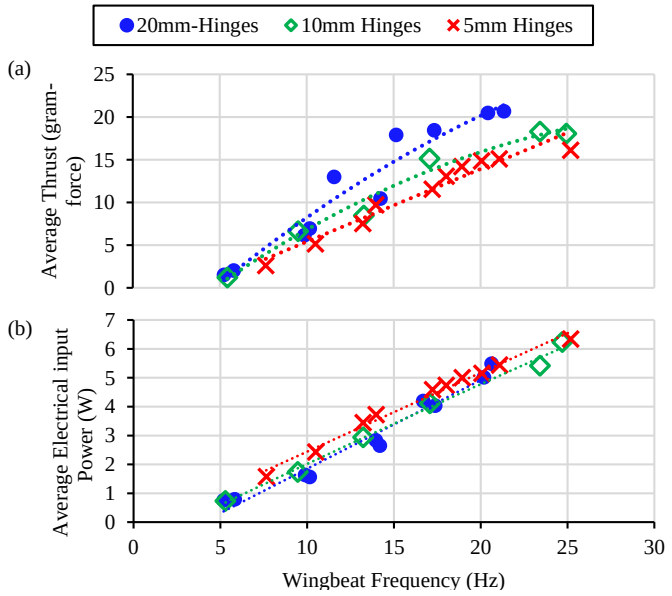

Figure 15 (a) Average thrust generation along wingbeat frequency. (b) Average electrical input power along frequency.

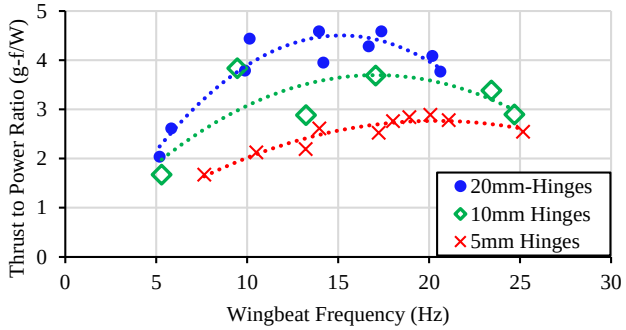

Figure 16 Ratio of the average thrust generation to the electrical power input to motor along frequency.

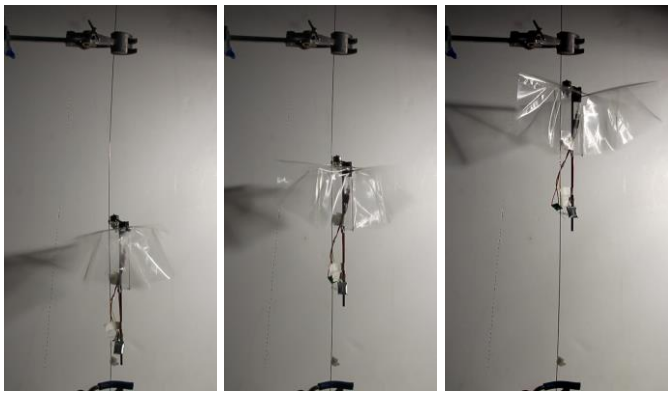

Figure 17 Photo of the 2cm hinges X-wing lifting its weight and climb in tethered flight demonstration.

5 CONCLUSION

We introduced an X-wing clapper mechanism integrated with elastic polyimide hinges to store sufficient elastic energy. The elastic polyimide hinges could store sufficient elastic energy for a large bending angle without breaking. This work shows that 4.2mJ elastic energy storage by using a polyimide film hinge is good at improving the energetic efficiency to 4.5 gram lift force per watt for the flapping 24cm-span X-wings. This present a 50% improvement of the maximum lift to power ratio as compared to that using a soft hinge of 0.8mJ. The X-13.4g wing clapper with matched elastic hinges is able to produce 20.7g thrust for lift off and climbing.

ACKNOWLEDGEMENTS

The authors wish to thank Temasek Laboratories @ National University of Singapore and Nanyang Technological University for their support of this project.

REFERENCES

[1] The Ornithopter Zone, "Full History of Ornithopters," [Online]. Available: http://www.ornithopter.org/history.full.shtml. [Accessed 2015].

[2] D. Lentink, S. Jongerius and N. Bradshaw, "The scalable design of flapping micro air vehicles inspired by insect flight," in *Flying insects and robots*, Springer-Verlag Berlin Heidelberg, 2009, pp. 185-205.

[3] K. M. E. De Clercq, "Flow Visualization and Force Measurements on a Hovering Flapping-wing MAV 'DelFly II'," Delft University of Technology, Delft, The Netherlands, 2009.

[4] R. Madangopal, Z. A. Khan and S. K. Agrawal, "Biologically Inspired Design Of Small Flapping Wing Air Vehicles Using Four-bar Mechanisms and Quasi-steady Aerodynamics," *Journal of Mechanical Design*, vol. 127, no. 4, pp. 809-816, 2005.

[5] S. S. Baek, K. Y. Ma and R. S. Fearing, "Efficient Resonant Drive of Flapping-Wing Robots," in *The 2009 IEEE/RSJ International Conference on Intelligent Robots and Systems*, St. Louis, USA, 2009.

[6] M. Keennon, K. Klingebiel, H. Won and A. Andriukov, "Development of the Nano Hummingbird: A Tailless Flapping Wing Micro Air Vehicle," in *60th AIAA Aerospace Sciences Meeting Including the New Horizons Forum and Aerospace Exposition*, Nashville, Tennessee, 9-12 January 2012.

[7] R. Wood, "Liftoff of a 60mg flapping-wing MAV," in *2007 IEEE/RSJ International Conference on Intelligent Robots and Systems*, San Diego, CA, USA, 2007.

[8] C. Richter and H. Lipson, "Untethered Hovering Flapping Flight of a 3D-Printed Mechanical Insect," in *12th International Conference on Artifical Lift (Alife XII)*, Odense, Denmark, 2010.

[9] F. v. Breugel, Z. E. Teoh and H. Lipson, "A Passively Stable Hovering Flapping Micro-Air Vehicle," in *Flying Insects and Robots*, Springer-Verlag Berlin Heidelberg, 2007, pp. 171-184.

[10] P. Zdunich, D. Bilyk, M. MacMaster, D. Loewen, J. DeLaurier, R. Kornbluh, T. Low, S. Stanford and D. Holeman, "Development and Testing of the Mentor Flapping-Wing Micro Air Vehicle," *Journal of Aircraft*, vol. 44, no. 5, pp. 1701-1711, 2007.

[11] R. Wood, "Design, fabrication, and analysis of a 3DOF, 3cm flapping-wing MAV," in *IEEE/RSJ International Conference on Intelligent Robots and Systems*, San Diego, CA, USA, 2007.

[12] R. Wood, R. Nagpal and G.-Y. Wei, Flight of the Robobees, Scientific American, March 2013.

[13] R. Sahai, K. C. Galloway, M. Karpelson and R. J. Wood, "A flapping-wing micro air vehicle with interchangeable parts for system integration studies," *2012 IEEE/RSJ International Conference onIntelligent Robots and Systems (IROS)*, pp. 501--506, 2012.